Journal of the Korean Nuclear Society
Volume 22, Number 2, June 1990

A Study on Effects of Axial Gas Flow in the Gap and Fuel Cracking on Fission Gas Release under Power Ramping

Jin Kyu Han* and Young Ku Yoon
Korea Advanced Institute of Science and Technology

(Received November 20, 1989)

출력 감발 조건하에서 핵분열 기체 생성물의 방출에 대한 축방향 기체 유동과 핵연료 파손의 영향에 관한 연구

한진규 · 윤용구
한국과학기술원

(1989. 11. 20 접수)

Abstract

The fission gas release model used in the SPEAR-BETA fuel performance code was modified by use of effective thermal conductivity for cracked fuel and by taking into account axial fission-gas mixing between the fuel-clad gap and the plenum. With use of this modified model the fission gas release was analyzed under various power ramping conditions of P_{max} and ΔP. Effective fuel thermal conductivity that accounts for the effect of fuel cracking was used in calculation of the fuel temperature distribution and the internal gas pressure under power ramping conditions. Mixing and dilution effects due to axial gas flow were also considered in computing the width and the thermal conductivity of the gap. The effect of axial gas flow was solved by the Crank-Nicholson method.

The finite difference method was used to save running time in the calculation. The present modified fission-gas release model was validated by comparing its predicted results with experimental data from various ramping tests in the literature and calculated results with use of the models used in the SPEAR-BETA and FEMAXI-IV codes. Results obtained with use of the present modified model showed better agreement with experimental data reported in the literature than those results with use of the latter codes. The fuel centerline temperature calculated with in troduction of effective thermal conductivity for centerline temperature calculated with introduction of effective thermal conductivity for cracked fuel was 200 higher fission gas release predicted with use of the modified model was nearly 6% larger on the average than that calculated by use of the unmodified model used in the SPEAR-BETA code.

요 약

SPEAR-BETA코드에서 사용된 핵분열 기체 방출 모델을 핵연료와 피복관 사이의 갭(gap)과 플레넘(plenum) 사이에서 축방향 핵분열 기체 혼합과 균열된 핵연료에 대한 유효 열전도도를 사용함으

*Presently with the Korea Power Engineering Company

로써 개량하여, P_{max}와 ΔP가 변하는 다양한 출력 감발 조건하에서 핵분열기체 방출 거동을 해석하였다. 핵연료 균열의 영향을 고려한 유효 열전도도는 핵연료의 온도 분포와 내부 기체 압력을 계산 하는데 사용되었고, 축방향 기체 유동으로 인한 혼합(mixing)과 희석(dilution) 효과는 갭의 폭과 열전도도를 해석하는데에 고려되었다. 축방향 기체 유동 효과를 계산하는데 있어서 계산속도를 빠르게 하기 위하여 유한차분법의 하나인 Crank-Nicholson 방법을 사용 하였다.

개량된 모델은 다양한 출력 감발 조건하에서 얻어진 실험 자료들과 SPEAR-BETA와 FEMAXI-IV 코드들에서 사용되는 모델들로부터 얻은 결과들을 비교함으로써 검증하였다. 개량된 모델의 결과는 위의 두 코드로부터 얻은 결과 보다는 실험 자료들과 잘 일치하였다. 균열된 핵연료에 대해 유효 열전도도를 사용하여 계산한 핵연료의 중심 온도는 균열되지 않은 핵연료의 경우에 비해 200℃ 정도 보다 높은 값을 나타냈고, 개량된 핵분열 기체 생성물의 분율은 SPEAR-BETA코드에서 얻은 값보다 평균 6% 정도가 높게 나타났다.

1. Introduction

Fission gases are produced within UO_2 pellets in LWR and released to the fuel-cladding gap by thermal diffusion due to temperature and concentration gradient. Since the thermal conductivities of fission gases are lower than that of helium filled initially in the gap, the release of fission gases results in a reduction of the thermal conductivity of the fuel-cladding gap and an increase of fuel temperature. The fission gas release also results in an increase of inner gas pressure and thus circumferential stress of the cladding.[1] The release of fission gases, however, depends on reactor's operating conditions such as power history including the power ramping rate. It has been reported that the release of fission gases under power ramping conditions is higher than that under normal steady-state operating conditions.[2]

There are many models proposed for the release of fission gases in LWR fuels. The fission gas release model used in the SPEAR-BETA fuel performance analysis code[3] consists of direct and indirect releases. The direct release is due to recoils of fission gases and sweeping of fission gases by grain-growth, while the indirect release is due to the thermal diffusion of fission gases to grain-boundaries and through open pores and fuel cracking. In both cases the fraction of fission gas release depends on fuel temperature and porosity.

For the SPEAR-BETA's fission gas release model it was assumed that a pressure equilibrium between pressures of the fuel-cladding gap and the fuel element's plenum occurs instantaneously. Under a transient condition or rapid power ramping conditions, however, the pressure equilibrium cannot be achieved instantaneously, although the amount of fission gas release into the fuel-cladding gap increases.[4] For the SPEAR-BETA's fuel temperature distribution model, the effect on thermal conductivity of fuel cracking was not taken into account. The SPEAR-BETA fuel performance analysis code developed for the Electric Power Research Institute (EPRI) comprises models for mechanistic fuel and cladding behaviors, their interaction, and mechanistic and statistical fuel failure. In the SPEAR-BETA code both mechanistic and statistical models for fuel failure are used in combination to improve the reliability of predicting fuel failure. Since the SPEAR-BETA is a comprehensive and useful code for analysis of light water reactors(LWR) fuel performance and predic-

tion of fuel failure probability, an attempt was made in the present study to improve the SPEAR-BETA's thermal conductivity and fission gas release models by taking into account effects of fuel cracking, and axial gas flow and mixing in the fuel-cladding gap under power ramping conditions.

To validate the present fission gas release model, the fraction of fission gas release was calculated for power ramping conditions and its results were compared with empirical data reported in the literature and with results obtained by use of the SPEAR-BETA code and the FEMAXI-IV code developed by the Japan Atomic Energy Research Institute (JAERI). The FEMAXI-IV is a computer code based on the finite element method for analysis of partial and comprehensive fuel element's behavior under steady or transient conditions.

Table.1 Fuel Element Properties

Fuel pellet		
	pellet type	PWR 16×16
	pellet radius(OD)	0.4579 cm
	grain size	6 μm
	theorical density	94%
	roughness	1 μm
Cladding		
	cladding material	Zircaloy-4
	cladding radius(OD)	0.5374 cm
	cladding radius(ID)	0.46475 cm
	roughness	1 μm
Gap width		68.5 μm
Plenum volume		2.2 cm^3
Fuel stack height		0.31 m
Fuel enrichment		3.1%

2. Effect of axial gas flow

Fission gases released to the fuel-cladding gap mix with the helium gas filled in the gap. Since the mole faction of fission gases becomes higher in the gap than in the plenum, gas flow through the gap to the plenum due to gradient in the axial direction occurs until an equilibrium between the pressures of the gap and the plenum is reached.[5] The time required to reach the pressure equilibrium between the gap and plenum depends on the gap width. For power ramping conditions, however, the gap width is narrowed due to pellet relocation, its difference in the thermal expansion of the fuel and cladding and fuel swelling on rapid power ramping. Because of this narrowed gap width the resistance to axial gas flow in the fuel-cladding gap increases and it requires a longer time to reach an equilibrium between the pressures of the gap and the plenum.[6] Until the pressure equilibrium in the gap and in the plenum is reached, the thermal conductivity of the gap in the case of slow gas flow model considered is lower than that of the plenum.

Table.2 Reactor Operating Conditions

Fuel burnup	2~31 GWD/MTU
Average linear heat rate	80~250 W/cm
Power increasing rate	100 W/cm/min
Maximum power level	395~525 W/cm
Duration of power ramping	24 hr

2.1 Derivation of equations for axial gas flow equilibrium in the gap

Fig.1 shows a schematic diagram of a fuel element and its subdivision axial zones for analysis of axial gas flow equilibrium in the fuel-cladding gap.

The mass balance equation at axial node j can be written[7] as

$$\frac{\partial}{\partial t}(\alpha_j \rho_j A_j)\Delta z_j + (\alpha \rho uA)_j - (\alpha \rho uA)_{j-1} = 0 \quad (1)$$

where j = number of axial nodes,

α_j = gas volume fraction at node j,

A_j = cross-sectional area at node j,

u_j = axial gas flow velocity at node j,

ρ_j =gas density at node j, and
Δz_j =distance along node j.

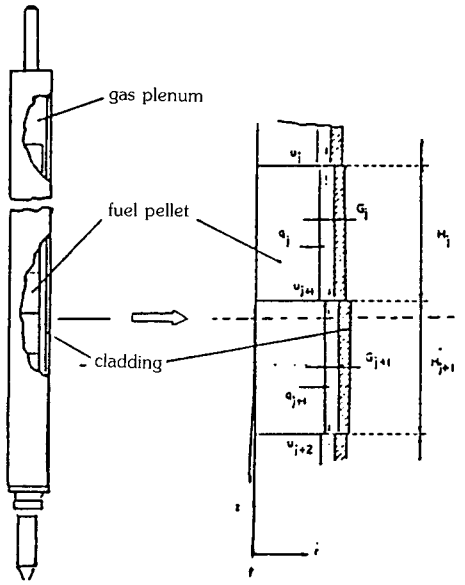

Fig.1 Fuel Rod Segmentation

The axial gas momentum balance equation provides the relationship that enables coupling of computational nodes. Hence a relationship between flow across a node boundary and pressure difference between node centers is derived. In the following it is assumed that the flow between nodes is friction-dominated. Momentum flux and density difference at different elevations, therefore, are neglected. For each half-node the momentum balance equation for the gas is expressed as :

$$(\alpha A)_j \frac{\Delta z_j}{2} \frac{\partial (\rho u)_j}{\partial t} + (\alpha A)_j P_{j+1/2} - (\alpha A)_j P_j = -K_j (\rho u)_j (\alpha A)_j \frac{\Delta z_j}{2} \quad (2)$$

and

$$(\alpha A)_{j+1} \frac{\Delta z_j}{2} \frac{\partial (\rho u)_{j+1}}{\partial t} - (\alpha A)_{j+1} P_{j+1/2} + (\alpha A)_{j+1} P_{j+1} = -K_{j+1} (\rho u)_{j+1} (\alpha A)_{j+1} \frac{\Delta z_{j+1/2}}{2} \quad (3)$$

where K_j=flow resistance factor at node j,
P_j=pressure at node j and
$P_{j+1/2}$=common interface pressure between half nodes.

The interface pressure $P_{j+1/2}$ can be eliminated by dividing each equation by its respective gas flow area and then by adding to give

$$\frac{\partial}{\partial t}\left[(\rho u)_j \frac{\Delta z_j}{2} + (\rho u)_{j+1} \frac{\Delta z_{j+1}}{2}\right] + (P_{j+1} - P_j) = -\left[K_j (\rho u)_j \frac{\Delta z_j}{2} + K_{j+1} (\rho u)_{j+1} \frac{\Delta z_{j+1}}{2}\right] \quad (4)$$

At the node interface, $(\rho u)_{j-} = (\rho u)_{j+}$, however, $(\alpha \rho u)_{j-} = (\alpha \rho u)_{j-}$. Multiplying the top and bottom of each flow term by the appropriate α, Equation (4) can be written as

$$\frac{\partial}{\partial t}\left[(\rho u)_j \frac{\Delta z_j}{2} \frac{\alpha_j}{\alpha_j} + (\rho u)_{j+1} \frac{\Delta z_{j+1}}{2} \frac{\alpha_{j+1}}{\alpha_{j+1}}\right] + (P_{j+1} - P_j) = -\left[K_j (\rho u)_j \frac{\Delta z_j}{2} \frac{\alpha_j}{\alpha_j} + K_{j+1} (\rho)_{j+1} \frac{\Delta z_{j+1}}{2} \frac{\alpha_{j+1}}{\alpha_{j+1}}\right] \quad (5)$$

$$\frac{\partial}{\partial t}\left[(\alpha \rho u)_j \frac{\Delta z_j}{2} \frac{1}{\alpha_j} + (\alpha \rho u)_{j+1} \frac{\Delta z_{j+1}}{2} \frac{1}{\alpha_{j+1}}\right] + (P_{j+1} - P_j) = -\left[K_j (\alpha \rho u)_j \frac{\Delta z_j}{2} \frac{1}{\alpha_j} + K_{j+1} (\alpha \rho u)_j \frac{\Delta z_{j+1}}{2} \frac{1}{\alpha_{j+1}}\right] \quad (6)$$

and then

$$\frac{\partial}{\partial t} (\alpha \rho u)_j \frac{1}{2}\left(\frac{\Delta z_j}{\alpha_j} + \frac{\Delta z_{j+1}}{\alpha_{j+1}}\right) + (P_{j+1} - P_j) = -(\alpha \rho u)_j \left[\frac{K_j \Delta z_j}{2 \alpha_j} + \frac{K_{j+1} \Delta z_{j+1}}{2 \alpha_{j+1}}\right] \quad (7)$$

The final equation is expressed as follows :

$$\frac{\partial}{\partial t} (\alpha \rho u)_j + \frac{P_{j+1} - P_j}{\Delta \bar{z}_j} = -\bar{K}_j (\alpha \rho u)_j \quad (8)$$

where $\bar{K}_j$=frictional flow resistance factor

$$= \left[\frac{K_j \Delta z_j}{2 \alpha_j} + \frac{K_{j+1} \Delta z_{j+1}}{2 \alpha_{j+1}}\right] / \Delta \bar{z}_j$$

and $\Delta \bar{z}_j$=effective axial node distance

$$= \frac{1}{2}\left(\frac{\Delta z_j}{\alpha_j} + \frac{\Delta z_{j+1}}{\alpha_{j-1}}\right)$$

Assuming at this stage that α and Δz along node are uniform, the axial gas momentum balance

equation can be written as

$$\frac{\partial}{\partial t}(\alpha\ \rho u)_j+\frac{P_{j+1}-P_j}{\Delta \bar{z}_j}=-K_{j+1/2}(\alpha\ \rho u)_j \qquad (9)$$

where $K_{j+1/2}=\frac{1}{2}(K_j+K_{j+1})$

and $\Delta \bar{z}_j=\frac{\Delta z_j}{\alpha_j}$

The flow resistance factor is obtained below on the basis of the Hagen-Poiseuille flow pattren for viscous flow in the thin hollow gap.[8]

$$K=\frac{H_a \mu}{2G^2} \qquad (10)$$

where H_a=Hagen number

$=22.0+0.24558/(40G-0.0007874)$,

G=gap width and

μ=gas viscosity.

Gas pressure is calculated from the ideal gas law equation

$$P=\rho R T \qquad (11)$$

From Eq.(9) the change of axial gas velocity at each node in time dt is calculated by use of the flow resistance factor of the gap in pressure gradient between each adjacent node as follows :

$$\frac{\partial u}{\partial t}=-\frac{1}{\rho_{gm}}\left\{\frac{\partial P}{\partial z}-H_a\frac{\mu}{2G^2}u\right\} \qquad (12)$$

The rate of the change of gas concentration at each node depends on gas diffusion due to axial concentration gradient and gas flow, and rate of fission – gas release from the UO_2 pellet. This can be expressed as

$$\frac{\partial \rho}{\partial t}+\frac{\partial}{\partial z}(\rho u)=\frac{\partial}{\partial z}\left\{D\frac{\partial \rho}{\partial z}\right\}+q \qquad (13)$$

where $\frac{\partial}{\partial z}\left\{D\frac{\partial \rho}{\partial z}\right\}$ = concentration change due to gas diffusion,

$\frac{\partial}{\partial z}\{\rho u\}$ = concentration change due to pressure gradient,

q=rate of fission gas release from the UO_2 pellet,

D=gas diffusion coefficient,

$\rho_{gm}=\rho$ M and

M=molecular weight of gas.

2.2 Evaluation of axial gas flow by the finite difference method

It is assumed that once fission gases are released into the gap, fission gas flow occurs in the axial direction only. Eqs.(11), (12) and (13) for gas pressure, change of axial gas velocity and gas concentration at each node, respectively, are further expressed by the Crank-Nicholson method.[9][10][11]

For node 1 Eg(14) is obtained :

$$\frac{1}{\Delta t}(u_1^{t+\Delta t}-u_1^t)=-\left\{(\rho_{gm})_{pl+1/2}^{t+\Delta t/2}\right\}^{-1}\cdot\left\{(H_{pl+1/2}^{t+\Delta t/2})^{-1}\cdot(P_{pl}^{t+\Delta t/2}-P_1^{t+\Delta t/2})+\frac{0.5H_{a\,pl+1/2}^{t+\Delta t/2}\mu_{pl+1/2}^{t+\Delta t/2}u_1^{t+\Delta t/2}}{(G_1^{t+\Delta t/2})^2}\right\} \qquad (14)$$

$$\frac{1}{\Delta t}\left\{(\rho)_1^{t+\Delta t}-(\rho)_1^t\right\}H_1^{t+\Delta t}G_1^{t+\Delta t}+\left\{\theta_1(\rho)_{pl}^{t+\Delta t/2}+(1-\theta_1)(\rho)_1^{t+\Delta t/2}\right\}u_1^{t+\Delta t/2}G_1^{t+\Delta t/2}$$

$$-\left\{\theta_2(\rho)_2^{t+\Delta t/2}+(1-\theta_2)(\rho)_1^{t+\Delta t/2}\right\}u_2^{t+\Delta t/2}G_{1+1/2}^{t+\Delta t/2}=q_1^{t+\Delta t/2}H_1^{t+\Delta t/2}G_1^{t+\Delta t/2}$$

$$+\frac{(D)_{pl+1/2}^{t+\Delta t/2}}{(H)_{pl+1/2}^{t+\Delta t/2}}\left\{(\rho)_{pl}^{t+\Delta t/2}-(\rho)_1^{t+\Delta t/2}\right\}G_1^{t+\Delta t/2}-\frac{(D)_{1+1/2}^{t+\Delta t/2}}{(H)_{1+1/2}^{t+\Delta t/2}}\left\{(\rho)_1^{t+\Delta t/2}-(\rho)_2^{t+\Delta t/2}\right\}G_{1+1/2}^{t+\Delta t/2} \qquad (15)$$

where H=height,

G=gap width, and

μ=gas viscosity for each node.

For node 2 to node N-1,

$$\frac{1}{\Delta t}(u_j^{t+\Delta t} - u_j^t) = -\left\{(\rho_{gm})_j^{t+\Delta t/2}\right\}^{-1} \cdot \left\{(H_{j-1/2}^{t+\Delta t/2})^{-1} \cdot (P_{j-1}^{t+\Delta t/2} - P_j^t) + \frac{0.5 f H_a {}_{j-1/2}^{t+\Delta t/2} \mu_{j-1/2}^{t+\Delta t/2} u_{j-1/2}^{t+\Delta t/2}}{(G_{j-1/2} l + \Delta t/2)^2}\right\} \quad (16)$$

$$\frac{1}{\Delta t}\left\{(\rho)_j^{t+\Delta t} - (\rho)_j^t\right\} H_j^{t+\Delta t} G_j^{t+\Delta t} + \left\{\theta_1(\rho)_{j-1}^{t+\Delta t/2} + (1-\theta_1)(\rho)_j^{t+\Delta t/2}\right\} u_j^{t+\Delta t/2} G_{j-1}^{t+\Delta t/2}$$

$$- \left\{\theta_2(\rho)_j^{t+\Delta t/2} + (1-\theta_2)(\rho)_{j+1}^{t+\Delta t/2}\right\} u_{j+1}^{t+\Delta t/2} G_j^{t+\Delta t/2} = q_j^{t+\Delta t/2} H_j^{t+\Delta t/2} G_j^{t+\Delta t/2}$$

$$+ \frac{(D)_{j-1/2}^{t+\Delta t/2}}{(H)_{j-1/2}^{t+\Delta t/2}}\left\{(\rho)_{j-1}^{t+\Delta t/2} - (\rho)_j^{t+\Delta t/2}\right\} G_{j-1/2}^{t+\Delta t/2} - \frac{(D)_{j-1/2}^{t+\Delta t/2}}{(H)_{j-1/2}^{t+\Delta t/2}}\left\{(\rho)_j^{t+\Delta t/2} - (\rho)_{j+1}^{t+\Delta t/2}\right\} G_{j+1/2}^{t+\Delta t/2} \quad (17)$$

where

$$\theta_1 = \begin{cases} 1\ , \text{ if } u_j^{t+\Delta t/2} > 0 \\ 0\ , \text{ if } u_j^{t+\Delta t/2} \le 0\ , \end{cases} \qquad \theta_2 = \begin{cases} 1\ , \text{ if } u_{j+1}^{t+\Delta t/2} > 0 \\ 0\ , \text{ if } u_{j+1}^{t+\Delta t/2} \le 0\ . \end{cases}$$

For node N,

$$\frac{1}{\Delta t}\left\{(\rho)_N^{t+\Delta t} - (\rho)_N^t\right\} H_N^{t+\Delta t} G_N^{t+\Delta t} + \left\{\theta(\rho)_{N-1}^{t+\Delta t/2} + (1-\theta)(\rho)_N^{t+\Delta t/2}\right\} u_N^{t+\Delta t/2} G_{N-1}^{t+\Delta t/2}$$

$$= \frac{(D)_{N-1/2}^{t+\Delta t/2}}{(H)_{N-1/2}^{t+\Delta t/2}}\left\{(\rho)_{N-1}^{t+\Delta t/2} - (\rho)_N^{t+\Delta t/2}\right\} G_{N-1}^{t+\Delta t/2} + q_N^{t+\Delta t/2} H_N^{t+\Delta t/2} G_N^{t+\Delta t/2} \quad (18)$$

where

$$\theta = \begin{cases} 1\ , \text{ if } u_N^{t+\Delta t/2} > 0 \\ 0\ , \text{ if } u_N^{t+\Delta t/2} \le 0 \end{cases}$$

For the gas plenum,

$$\frac{1}{\Delta t}\left\{(\rho)_{pl}^{t+\Delta t} - (\rho)_{pl}^t\right\} V_{pl}^{t+\Delta t/2} - \left\{\theta(\rho)_{pl}^{t+\Delta t/2} + (1-\theta)(\rho)_1^{t+\Delta t/2}\right\} u_1^{t+\Delta t/2} G_1^{t+\Delta t/2}$$

$$= \frac{(D)_{pl+1/2}^{t+\Delta t/2}}{(H)_{pl+1/2}^{t+\Delta t/2}}\left\{(\rho)_{pl}^{t+\Delta t/2} (\rho)_1^{t+\Delta t/2}\right\} G_1^{t+\Delta t/2} \quad (19)$$

where

$$\theta = \begin{cases} 1\ , \text{ if } u_1^{t+\Delta t/2} > 0 \\ 0\ , \text{ if } u_1^{t+\Delta t/2} \ge 0 \end{cases}$$

The convergence is checked

$$\left| \frac{(\rho_j)' - (\rho_j)^{t+\Delta t}}{(\rho_j)^{t+\Delta t}} \right| < \varepsilon \quad (20)$$

where ε = limit value of the relative error (= 0.005)

$(\rho_j)^{t+\Delta t}$ = gas concentration computed at node j

$(\rho_j)'$ = gas concentration supposed at node j

2.3 Numerical calculation procedure for axial gas flow

The procedure for numerical calculation of axial gas flow is as follows:

(1) input the values of fuel stack height, gap width, plenum volume and gas density(Table 1),

(2) supposition of the gas density at each node and time $t+\Delta t$,

(3) calculation of the gas flow velocity u_j at each node and time $t+\Delta t$,

(4) calculation of the gas density at each node and time $t+\Delta t$ with use of Eqs.(15), (17), (18) and Eq.(19),

(5) convergence check in the gas density calculation with use of Eq.(20) and iteration of step (3) until the calculated gas density is converged.

(6) calculated results of the gas density and the gas pressure are used for calculation of the fuel-cladding gap conductance.

3. Effect of fuel cracking on thermal conductivity

The heat conduction equation appropriate for fuel pellets under power ramping is given by the following equation[12]:

$$\frac{1}{r}\frac{\partial}{\partial r}\left(rK\frac{\partial T}{\partial r}\right)+H=\rho C_p\frac{\partial T}{\partial t} \tag{21}$$

where T(r,t)=fuel temperature(℃),

H(r,t)=volumetric heat generation rate(W/cm^3),

K(r,t)=fuel's thermal conductivity(W/cm^2. ℃),

C_p(r,t)=fuel's heat capacity(kJ/kg.℃),

ρ =fuel density(kg/m^3),

r=pellet radius(m) and

t=time(sec).

1) Thermal conductivity of uncracked fuel[13]

The thermal conductivity of UO_2 fuel depends on fuel temperature and its porosity. An empirical correlation used for the thermal conductivity of UO_2 fuel that varies with temperature and porosity factor is given as

$$K_f=K_p\{6.43-4.93\times10^{-3}T+1.455\times10^{-6}T^2\} \tag{22}$$

where K_p=porosity form factor

$=1-0.971p+6.06p^2$ and

p=porosity fraction.

2) Thermal conductivity of cracked fuel

Since the thermal conductivity of fuel with cracks is lower than that of uncracked fuel, the thermal conductivity of cracked fuel was calculated with use of a correction factor(K_c) for which the effect of fuel cracking is taken into account, modifying the thermal conductivity of uncracked fuel.

The correction factor(K_c) is computed by the empirical correlation[14]

$$K_c=1-C\cdot C_{rel}\left\{1-\frac{K_g}{K_f}\right\} \tag{23}$$

where C=correlation constant,

C_{rel}=increased rate of pellet radius due to fuel cracking

$$=\frac{V_c\cdot R_f}{3.2\times10^{-4}},$$

V_c=fraction of volume inrcement due to fuel cracking($\Delta V/V$),

R_f=as-fabricated pellet radius and

K_f=gas conductivity in the fuel-cladding gap.

Then the thermal conductivity of cracked fuel is

$$K_{eff}=K_f\cdot K_c \tag{24}$$

4. Results and Discussion

A procedure is required to confirm the validity of the present modified fission gas release model. The model's validation is accomplished by comparison of the results obtained by use of the present modified code with experimental data reported previoulsy[15] and also with results obtained by use of the JAERI's FEMAXI-IV code[17] and EPRI's SPEAR-BETA Code. Fig.2 shows the com-

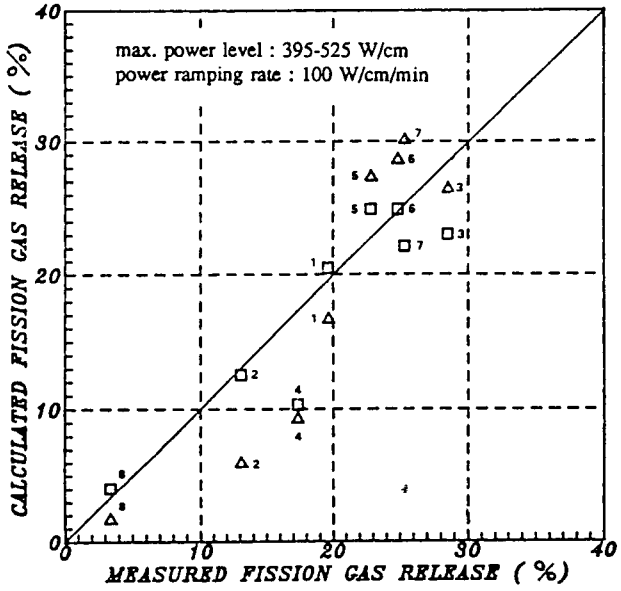

Case	P_{max}	ΔP
1	490	190
2	445	140
3	530	230
4	440	140
5	488	188
6	487	187
7	525	225
8	378	78

Unit : W/cm

Fig.2 The Fractions of Fission Gas Release Computed with Use of Modified SPEAR-Model and Unmodified FEMAXI-IV Model :
□ : results from the modified SPEAR-BETA model
△ : results from the unmodified FEMAXI-IV model.
The numbers denote cases for power-ramping conditions.

parison of the above-mentioned calculated results and experimental data under conditions of P_{max} and ΔP. The relative error of the results obtained by use of the modified code and the FEMAXI-IV code was 6.8% and 11.4%, respectively, from the experimental values of fission gas release.

Fig.3 shows the comparison of the fractions of fission gas release calculated with use of the present modified model with the unmodified SPEAR-BETA's fision gas release model and experimentally observed values under various power ramping conditions. The fractions of fission gas release calculated with use of the present modified model were 10% higher on the average in comparison with those calculated with use of the unmodified model, and the former agree with experimental results better than the latter.

BETA's

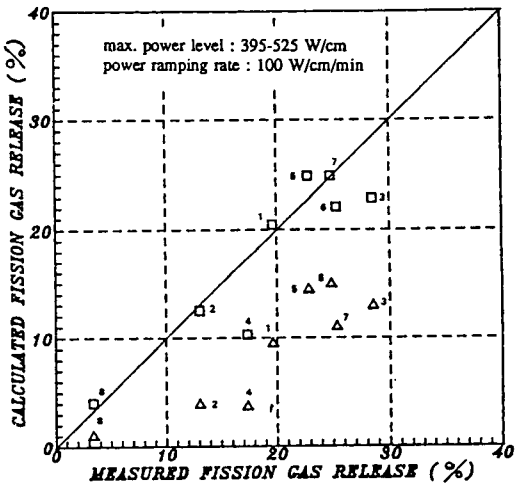

Fig.3 The Fractions of Fission-Gas Release Computed with Use of the Modified and Unmodified SPEAR-BETA's Model :
□ : results from the modified model
△ : results from the unmodified model.

Fig.4 shows the centerline temperatures of the fuel calculated with use of the heat conduction model for uncracked fuel and the modified heat-conduction model for cracked fuel when the linear heat rate of 490 W/cm/min. Fig.5 whows the radial temperature distribution within the fuel calculated with use of the unmodified model for uncracked and the modified model for cracked fuel when the above-mentioned linear heat rate was maintained. Fuel thermal conductivity at certain radial position depends on fuel temperature and its porosity factor. Since fuel cracking and relocation of fuel pellet fragments occur under power ramping conditions, the open space in the

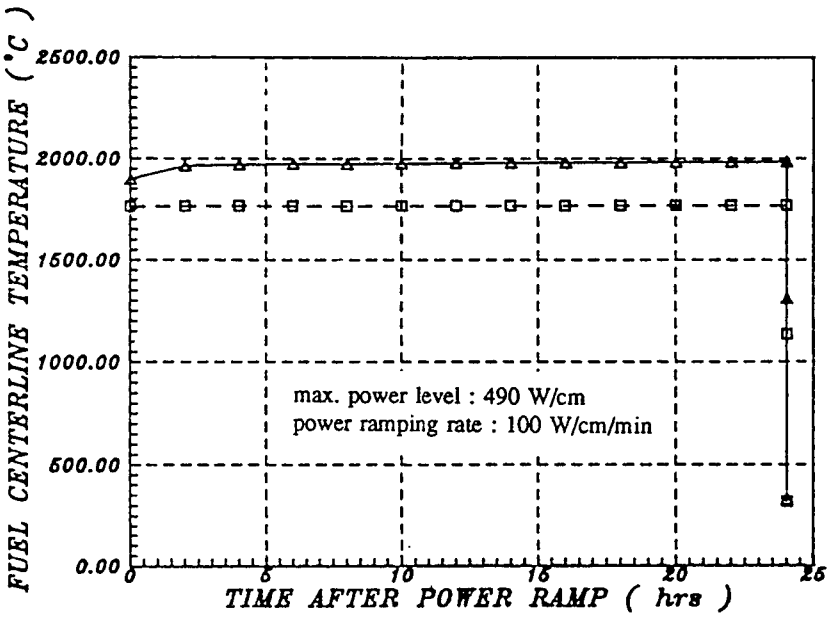

Fig.4 Fuel Centerline Temperatures vs Holding Time after Power Ramping Calculated with and without Use of An Effective Thermal Conductivity for Cracked Fuel :

□ : results from use of thermal conductivity for uncracked fuel

△ : results from use of effective thermal conductivity for cracked fuel.

cracked fuel and the volume of the fuel pellet increase on power rise. Consequently, the effect on thermal conductivity of fuel cracking is taken into account and this results in lowering the thermal conductivity of the fuel pellet according to Eq.(16). When cracking of fuel occurs under power ramping conditions, fuel thermal conductivity decreases because gaps between cracks are wider due to smaller fuel thermal expansion for a lower temperature distribution. As can be seen in Fig.4, the fuel centerline temperature calculated with use of the modified heat conduction model for cracked fuel was approximately 200℃ higher than that calculated with use of the modified heat conduction model for uncracked fuel.

Fission gases are released to the gap between the fuel pellets and cladding due to thermal diffusion at a high linear heat rate after a power ramping, and this results in an increase of the fraction of fission gas release in the gap. When fission gases are released, axial gas flow from the gap to the plenum occurs due to increasing gas

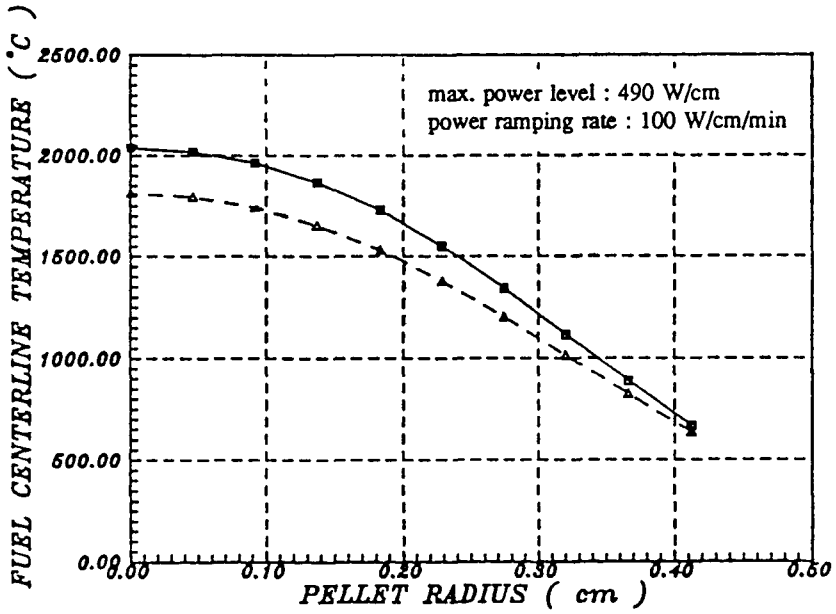

Fig.5 Radial Fuel Temperature Distributions Calculated with Use of Effective Thermal Conductivity for Cracked Fuel and Thermal Conductivity for Uncracked Fuel :

□ : results from use of effective thermal conductivity·

△ : results from use of thermal conductivity.

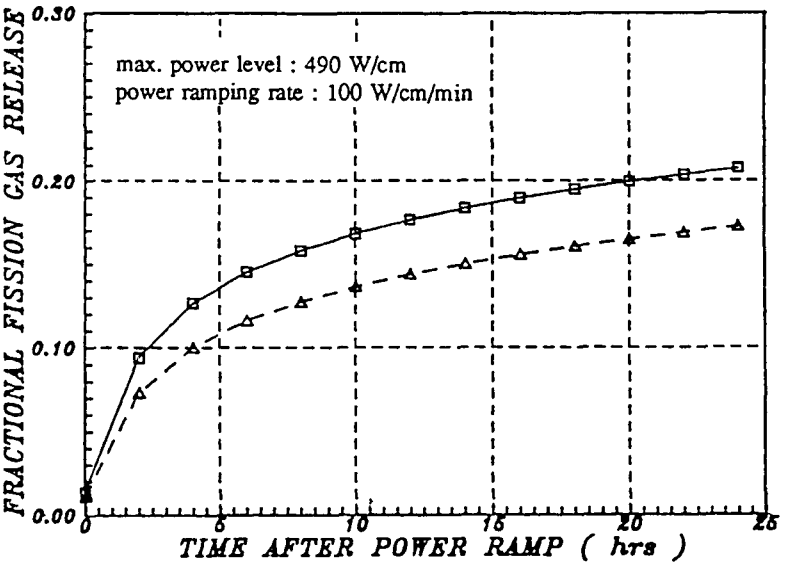

Fig.6 Fractional Fission-Gas Release vs Holding Time after Power Ramping Calculated with Use of The Unmodified and Modified SPEAR-BETA Models :

□ : results from use of the modified model

△ : results from use of the unmodified model.

pressure gradient until an equilibrium pressure is reached. Two fission-gas release models with and without axial gas flow under the same power ramping condition were compared to analyze its effects on fission gas release. It was assumed for the unmodified fission gas model without axial gas flow that an equilibrium between the pressures of the gap and the plenum occurs instantaneously. Fig.6 shows the fractions of fission gas release calculated with use of the two models. The fractions of fission gas release calculated with use of the modified model with axial gas flow was 6% higher than that calculated with use of the unmodified model. The gap width of the fuel rods on rapid power rise decreases due to the difference in thermal expansion of the fuel and claddding, fuel swelling, and relocation of cracked fuels. As the gap width decreases, the resistance to axial gas flow in the gap becomes greater, and this results in a higher gas pressure in the gap than in the plenum until an equilibrium is reached between the pressures of the gap and the plenum. Hence the thermal conductivity of the gap decreases, and the fuel temperature increases. This results in an increase of fission gas release.

5. Conclusions

1) It was possible to modify the fission gas release model used in the EPRI's SPEAR-BETA Fuel Performance Code by taking into account the effect of axial gas flow and mixing in the fuel-cladding gap under power ramping conditions.
2) Effective thermal conductivity that accounts for the effect of fuel cracking under power ramping was used for the heat conduction model to determine the fuel temperature distribution.
3) The fuel-temperature distribution determined by use of the effective thermal conductivity yielded the fuel centerline temperature that is 200℃ higher than that calculated with use of the unmodifided thermal conductivity for uncracked-fuel.
4) The fraction of fission-gas release computed with use of the present modified model was about 6% greater than that computed with use of the unmodified SPEAR-BETA fission gas release model.

References

1. T. Nakajima, "FEMAXI-IV : A Computer Code for The Analysis of Fuel Rod Behavior under Transient Conditions," Nucl. Eng. and Design, Vol.88, 69-84(1985)
2. P. Kunsen, "Evaluation of LWR Fuel Performance under Transient and Off-normal Conditions, A Review of Recent Reports," Riso National Laboratory, Denmark(1979)
3. R. Christensen et al., "SPEAR-BETA Fuel Performance Code System-Volume.1 : General Description," EPRI Final Report NP-2291(1982)
4. H. Sakagauri et al., "BEAF-A Computer Program for Analysis of Light Water Reactor Fuel Rod Behavior," Nucl. Eng. and Design., Vol.86, 241(1985)
5. D.D. Rowe and R.N. Oehlberg, "An Analytical Model for Transient Gas Flow in Nuclear Fuel Rods," Nucl. Tech., Vol.54, 174(1981)
6. S.J. Dagbjartsson et al., "Axial Gas Flow in Irradiated PWR Fuel Rods," TREE-NUREG-1158, Idaho National Eng. Laboratory(1977)
7. E.R.G. Eckert et al., "Analysis of Heat and Mass Transfer," McGraw-Hill Book Company, U.K. 700(1972)
8. K.R Cho et al., "Fluid Dynamics," Kae Mun Sa, 296(1984)
9. F.H. Harlow et al., "A Numerical Fluid Dynamics Calculation Method for All Flow Speeds," J. Compt. Phys. Vol.8,197(1971)
10. C.H. Kim, "Numerical Methods and Computer Programming," Kyo Hak Sa(1984)

11. Carnahan et al., "Applied Numberical Method," John Wiley and Sons, New York(1969)
12. M.M. El-Wakil, "Nuclear Heat Transport," International Book Company, Toronto, 203(1971)
13. L.J. Siefken et al., "FRAP-T6 : A Computer Code for The Transient Analysis of LWR Fuel Rod Behavior," NUREG/CR-2148, U.S. Nuclear Regulatory Commission(1979)
14. A. Biandreria, "The Effect of Porosity on Thermal Conductivity of Ceramic Bodies," Trans. ANS., Vol.9, 15(1966)
15. H. Mogard et al., "The International Over-Ramp Project at Studsvik," Presented at ANS Topical Meeting(1982)
16. R. Thomas, "The Studsvik Inter-Ramp Project : An International Power Ramp Experimental Program," J.of Nucl. Mat. Vol.87, 215(1979)
17. T. Nakajima and H.Saito, "A Comparison between Fission Gas Release Data and FEMAXI-IV Code Calculation," Nucl. Eng. and Design, Vol. 101, 267(1987)